

Structural stability of phases of black phosphorus

K. J. Chang and Marvin L. Cohen

Department of Physics, University of California, Berkeley, California 94720
and Materials and Molecular Research Division, Lawrence Berkeley Laboratory, Berkeley, California 94720
(Received 20 December 1985)

The pseudopotential method is used to examine the structural stability of high-pressure orthorhombic, rhombohedral (*A-7*), and simple cubic (sc) phases of black phosphorus. The calculated ground-state properties are in good agreement with the measured values for each phase. A total-energy study gives the orthorhombic phase as the most stable structure at low pressures. At higher pressures it transforms into the *A-7* structure in agreement with experiment. At even higher pressure, the calculations indicate that the *A-7* phase is stable with respect to the sc structure as is the case for other group-V elements. Measurements show that the sc phase is stable at 110 kbar at room temperature. This suggests that the calculated crystal energy for the *A-7* phase is too low and it requires a finite energy shift. With an *a priori* energy shift, the transition pressure and volume are in good agreement with experiment. A possible source of this correction is the zero-point energy or temperature renormalization of the phonon frequencies caused by anharmonicity. The changes of the energy band structures and charge densities for the *A-7* displacement and selected phonon frequencies are calculated.

I. INTRODUCTION

There have been several stimulating theoretical and experimental studies of black phosphorus (P) subjected to high pressures. A reversible structural sequence from the orthorhombic to rhombohedral (arsenic or *A-7*) to the simple cubic (sc) structure was observed at room temperature in black phosphorus.¹⁻³ The crystal phases stabilized at low pressure show very anisotropic properties in atomic bonding,⁴ resistivity,⁵ and lattice compressibility.^{3,4} Furthermore, recent observations^{6,7} of an anomalously high superconducting transition temperature in the high-pressure modifications of black phosphorus provide added motivation to study this material.

The orthorhombic structure of black phosphorus is semiconducting and the most stable form at normal pressure.¹⁻⁴ The puckered layers existing in this phase have two different bond characteristics:^{2,4} the covalent intralayer bonding and weak van der Waals bonding between layers. The different bonding nature results in various anisotropic features in the resistivity and lattice compressibility. With increasing pressure, the distances between puckered layers decrease faster than intraplane separations because of their weaker coupling. The crystal structure then changes into the *A-7* phase at pressures ranging from 40 to 80 kbar (Refs. 1-6). The *A-7* phase is semimetallic and is similar in many respects to the group-V elements⁸ As, Sb, and Bi. The rhombohedral structure can be formed from the sc phase by an internal displacement of the atomic lattice, accompanied by a rhombohedral distortion.⁸ The pressure for the *A-7* to sc transformation in black phosphorus was found to be 110 kbar at room temperature.^{1,3} The sc phase is a nondense packing structure and only found to be stable in single polonium crystals.⁹ In the group-V materials, the pressure-induced *A-7* to sc distortion was also found¹⁰ in antimony

(Sb) at 70 kbar. In contrast, in Bi the *A-7* structure (Bi I) was found¹¹ to transform to a monoclinic structure (Bi II) at 25.5 kbar.

There have been a few theoretical studies on the phase stability of black phosphorus. Previous pseudopotential band-structure calculations¹² showed that the *A-7* phase in the group-V elements is an energetically more favorable structure than the sc structure because of a lowering of the band-structure energy. The *A-7* distortion breaks a crystal symmetry and thus induces a band separation between bonding and antibonding *p* states in the sc phase. Although the model of the band splitting arising from the *A-7* distortion gives some insight into understanding the phase stability, it is still only a qualitative explanation. More quantitative calculations¹³ based on the local pseudopotential method were attempted for various crystal structures. These calculations performed at zero temperature were successful in explaining the stability of the *A-7* phase with respect to the sc; however, they failed in finding the stable orthorhombic phase at normal pressure. A likely limitation in these studies is the fact that the calculations are based on second-order perturbation theory and there are significant higher-order energy terms when comparing black phosphorus with five valence electrons per atom to silicon with four valence electrons.

In this paper we present the results of *ab initio* pseudopotential calculations of the structural stability of high-pressure black phosphorus. The calculated lattice constants, bulk moduli, and the pressure derivative of the bulk moduli are compared with experiments for the orthorhombic, *A-7*, and sc phases. The pressure-induced solid-solid phase transitions are also investigated. To understand the structural stability between the *A-7* and the sc structures, we study the band structure and charge distribution for each phase. The phonon frequency associated with the *A-7* internal displacement of the sc struc-

ture is found to be very soft and thus the sc structure is unstable.

In Sec. II we discuss the method used and the accuracy of the calculation. Section III describes the crystal structures. In Sec. IV the results of the calculations for the structural properties are presented and discussed. The changes of the band structure, charge density, and phonon frequencies for the *A-7* distortion are also discussed. In Sec. V concluding remarks are made.

II. METHOD

The pseudopotential-total-energy method¹⁴ is used to investigate the structural properties within the local-density-functional theory.¹⁵ The exchange and correlation functional is approximated by the use of the Wigner interpolation formula.¹⁶ The calculations are done at zero temperature. The total-energy method using *ab initio* pseudopotentials has been successful in predicting the cohesive and dynamical properties for solids ranging from metals to insulators. However, the calculations for insulators have focused mostly on systems with an average atomic valence of four electrons: for example, the group IV (C, Si, and Ge),^{17,18} the group III-V (GaAs, GaP, AlAs, and AlP),^{19,20} the group II-VI (BeO and MgO),^{21,22} and the group I-VII (NaCl and KCl).²³

The *ab initio* pseudopotentials are generated²⁴ with separate nonlocal components having *s*, *p*, and *d* symmetry. Because of the relatively low atomic number of phosphorus, for both atomic and solid-state calculations relativistic and spin-orbit-coupling effects are not included. Recent *ab initio* pseudopotential calculations²⁵ have shown that even for heavier atoms neglecting the spin-orbit coupling does not affect the calculated ground-state properties significantly. This was tested for SnTe and PbTe with an average of five valence electrons per atom.

The crystalline total energies are calculated self-consistently in momentum space.²⁶ A plane-wave basis set with a kinetic energy cutoff of 11.5 Ry [this cutoff was also used for Si (Refs. 18 and 27)] is used to expand the wave functions. Because of the semimetallic and metallic behavior^{1,2,5} of black phosphorus at high pressures, uniform grids of a *k*-point set are used for the summation over the Brillouin zone. This set of *k* points actually avoids high symmetry points and thus gives an unprejudiced representation of the Fermi surface.²⁸ Grids of 6, 60, and 165 sampling points in the irreducible Brillouin zone are chosen for orthorhombic, rhombohedral, and simple cubic, respectively. The total energy is found to be stable to within 0.5 mRy per atom.

For the orthorhombic phase,¹⁻³ the total energies are optimized by varying the atomic parameters, *u* and *v*, and the ratio of the lattice constants, *a*, *b*, and *c*, while keeping the volume fixed. The total energies for the *A-7* phase are also optimized by changing the internal lattice displacement τ and the rhombohedral distortion angle α . In this case, the Hellmann-Feynman forces²⁹ are computed and used to find optimum configurations in the structures.

The total energies are calculated as a function of volume for various structural types, and then fitted to the

Murnaghan equation of state.³⁰ Then, the ground-state properties, such as equilibrium lattice constant, bulk modulus (B_0), and the pressure derivative of bulk modulus (B'_0), can be obtained. The differences of the crystal energies among the structures are used to distinguish the structural stability at various pressures, and then to predict the transition pressures and volumes for solid-solid phase transitions.

The calculations for the phonon frequencies are done for the modes at high symmetry points along the [111] direction in the Brillouin zone of the sc phase. With the use of the frozen-phonon approximation,³¹ we estimate the phonon frequencies from the energy difference between the undistorted and distorted lattices. We also calculate anharmonic terms³² in the phonon couplings which are responsible for the temperature renormalization of the frequency. By expanding the change of the crystal energy in terms of the phonon displacement, the fourth-order terms, corresponding to the phonon-phonon interaction, are calculated within the frozen-phonon approximation.

III. CRYSTAL STRUCTURES

Black phosphorus remains in the orthorhombic form¹⁻⁴ up to 40–80 kbar with space group D_{2h}^{18} . This crystal structure has eight atoms in the unit cell and consists of puckered layers^{2,4} which are shown in Fig. 1. Within the layers, each atom forms three covalent bonds containing the $3p$ electrons. The layers are connected by weak van der Waals forces. Because of the different bonding in the orthorhombic structure, the interlayer distance is much larger than the intralayer bond lengths; the interlayer distance is $b/2=5.239$ Å and the intralayer lengths are 2.224 and 2.244 Å at normal pressure.² The atomic parameters, *u* and *v*, specify the atomic coordinates in the orthorhombic structure. The atoms are located at the following points:

$$\begin{aligned} &\pm(0, vb, uc), \quad \pm[a/2, -vb, (u + \frac{1}{2})c], \\ &\pm[a/2, (v + \frac{1}{2})b, uc], \quad \pm[0, (\frac{1}{2} - v)b, (u + \frac{1}{2})c]. \end{aligned}$$

Figure 2 shows adjacent puckered layers projected onto

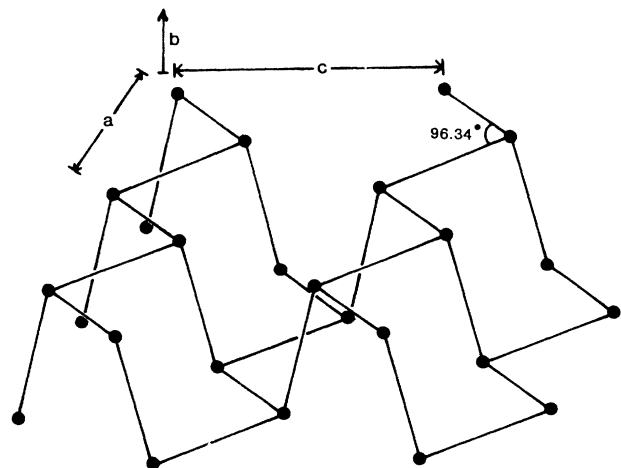


FIG. 1. Puckered layer of orthorhombic black phosphorus.

the (100) plane. When the pressure increases, the van der Waals bonds are shortened while the covalent bonds change slightly. Furthermore, because of weak restoring forces between the puckered layers, the layers will experience a shear motion. After the combined motions of lattice compression and layer sliding, the orthorhombic structure displacively changes into the rhombohedral phase as illustrated in Fig. 2. The sliding motion of the layers is similar to those found in the graphite to diamond transition³³ in C and the primitive hexagonal to hexagonal closed-packed transition²⁷ in Si. When the interlayer distance of the orthorhombic structure is shortened by pressure, the shear motion of the layers by $a/2$ relative to its adjacent layers increases the chance for atoms in different layers to form new covalent bonds connected by dashed lines in Fig. 2. Actually, the rhombohedral structure is formed by local atomic rearrangements of u and v .

The rhombohedral structure with space group D_{3d}^6 differs from the simple-cubic structure by a rhombohedral ($A-7$) distortion and an internal displacement of the lattices along the diagonal axis of the cube. The $A-7$ distortion is determined by the shear angle α between the primitive translation vectors. The internal displacement is characterized by the separation $2\tau=2ud$ of two interpenetrating face-centered lattices where d is the diagonal of the rhombohedral lattice. When $u=0.25$ and $\alpha=60^\circ$, the structure corresponds to the simple-cubic structure.

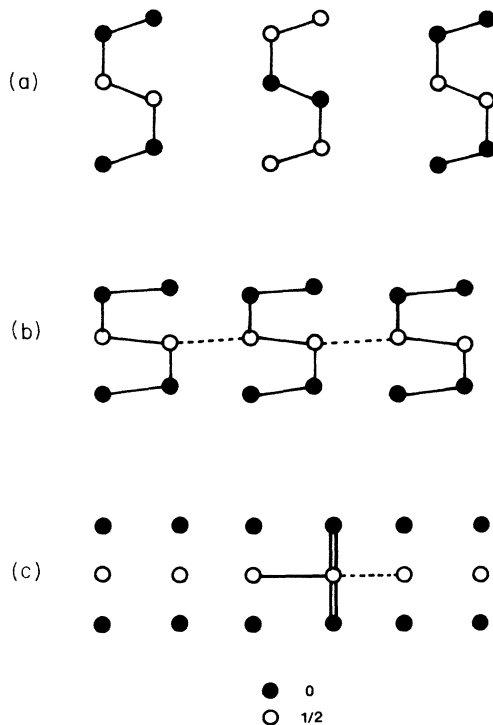


FIG. 2. Puckered layers projected onto the (100) plane for (a) orthorhombic at normal pressure, (b) a compressed volume along the b axis together with a decreasing of u and increasing of v (see text), and (c) sc with $u=0$ and $v=0.125$. In (b) and (c), the dashed lines denote new covalent bonds between adjacent layers. An octahedral bond is shown in (c). Numbers denote the fractional displacements out of the plane in units of a .

In Fig. 2 the simple-cubic structure is successively obtained from the orthorhombic structure through $A-7$ by setting $a=c=b/(2\sqrt{2})$.

IV. RESULTS

A. Ground-state properties

The calculated results for the ground-state properties, equilibrium lattice constant, bulk modulus, and pressure derivative of the bulk modulus are summarized and compared with experiment in Table I for the orthorhombic, rhombohedral, and simple-cubic structures of black phosphorus. Equilibrium volumes for each phase are in good agreement (within 2.5%) with the measured values. This discrepancy in the volumes corresponds to 0.8% error for the averaged lattice constants. The experimental volumes for the high-pressure $A-7$ and sc phases are obtained by fitting the data to the Murnaghan equation.

For the orthorhombic structure, the lattice parameters a , b , and c and atomic parameters u and v are obtained by optimization through the use of calculated Hellman-Feynman forces. Their values agree well with the measurements. With increasing pressure, we find that the lattice parameter a , along which two covalent bonds are in close proximity, changes very slowly while the interlayer parameter b and the parameter c containing the other covalent bond decrease faster. As a consequence, the linear compressibility κ_l is very anisotropic as discussed in Sec. III. From Fig. 3, we estimate $\kappa_l \sim 10^{-3} \text{ kbar}^{-1}$ for the directions b and c and $10^{-4} \text{ kbar}^{-1}$ along axis a , respectively. These values for κ_l 's are close to the measured values.^{3,4} Since the layers are stacked via weak van der Waals forces, the linear compressibility along the interlayer direction is relatively large. However, it is peculiar that κ_l along the a axis is much smaller than that in the c direction within the layers. The anisotropy in the stiff-

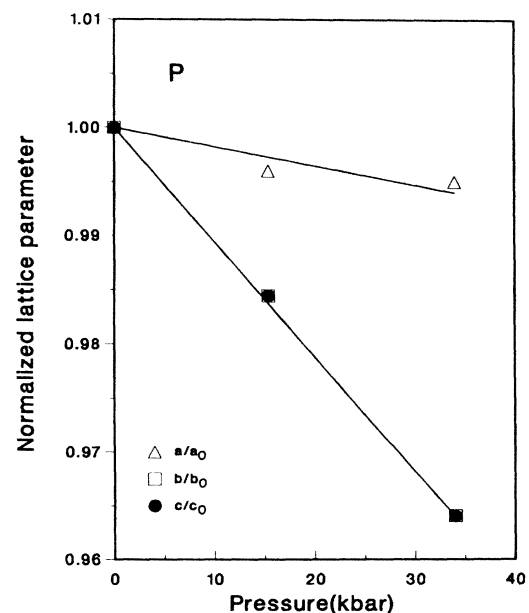


FIG. 3. Calculated lattice parameters versus pressure for the orthorhombic structure. Lattice parameters are normalized by their values at zero pressure.

TABLE I. Comparison with experiment of the calculated equilibrium lattice constants, bulk moduli, and pressure derivatives of the bulk moduli for the orthorhombic, *A*-7, and sc structures of black phosphorus. The equilibrium volumes and lattice constants are in units of \AA^3 per atom and \AA , respectively. The bulk moduli are in units of kbar. The atomic parameters u and v (at 0 kbar) are for the orthorhombic and the internal displacement u and rhombohedral angle α (at 97 kbar) are for the *A*-7 structure, respectively.

	Volume	a	b	c	$u(u)$	$v(\alpha)$	B_0	B'_0
				Orthorhombic				
Calc.	19.432	3.339	10.610	4.388	0.0840	0.1020	326	5.55
Expts.								
(Ref. 2)	18.993	3.3136	10.478	4.3763	0.0806	0.1017		
(Ref. 3)							360±20	4.5±0.5
(Ref. 4)	18.973	3.3133	10.473	4.374	0.0806	0.1034	325.3	6.11
				<i>A</i> -7				
Calc.	16.939				0.230	57.21	593	3.31
Expts.								
(Ref. 1)					0.21–0.22	57.25		
(Ref. 3)	16.6±0.2				0.228		460±40	3.0±0.6
				sc				
Calc.	15.5816	2.4977					956	3.1
Expt. (Ref. 3)	15.2±0.2	2.4771					950±50	2.1±0.8

ness of the layer results from the different geometries of the covalent bonds surrounding each atom. When compressed in direction a , two covalent bonds produce a strong repulsive Coulomb interaction since the bonds making a bond angle of 96.34° (Ref. 2) at normal pressure are very close (see Figs. 1 and 5). In direction c the covalent bond is relatively far from the other two along the a axis and thus a compression does not produce such a strong restoring force. In addition, the atomic parameter u is found to decrease while v increases with pressure. This fact is also consistent with experiment.⁴ In fact, the decrease of the parameters b and c brings the orthorhombic structure² ($c/a=1.314$ and $b/a=3.177$ at normal pressure) closer to the sc structure. Moreover, the sc structure corresponds to $u=0$ and $v=0.125$ as shown in Fig. 2.

For the rhombohedral structure, the calculated internal displacement u and rhombohedral angle α are in good agreement with the measured values.^{1,3} The group-V materials³⁴ tend to have decreasing values of u and α in going from Bi to As because of the increasing covalency in the bonding. In black phosphorus, the values of u and α for the *A*-7 structure are similar to those in Bi rather than Sb and As. With increasing pressure, the parameters u and α increase as seen in Bi, Sb, and As and then the deviations from the sc lattice decrease. However, they are still smaller than those corresponding to the sc structure.

The calculated bulk modulus and pressure derivative of the bulk modulus are in good agreement with the measured values.³ As seen in Table I, the bulk modulus increases as the phase changes from orthorhombic to *A*-7 to sc. Since the orthorhombic structure is in a layer structure, its bulk modulus, representing the curvature of the total-energy curves in Fig. 4, is the smallest.

The cohesiveness for each phase plays an important role in determining its structural stability. In the next section we discuss the structural stability of highly condensed black phosphorus and the pressure-induced structural transformations.

B. Phase stability of black phosphorus

For the group-V elements, some structural regularities¹² have been suggested as in the case of materials with average atomic valence four. Based on bond and band arguments,³⁵ the group-IV, -(III-V), and -(II-VI) semiconductors favor tetrahedrally coordinated structures, e.g., diamond, zinc blende, and wurtzite, primarily because of sp^3 hybridization in the bonding. In the group-V elements, the bonding and antibonding s states are completely occupied because the s electrons are deeply bound. The chemical bonds in this group are determined mainly by the $3p$ orbitals and thus favor the structures that are octahedrally coordinated like the simple-cubic and distorted-simple-

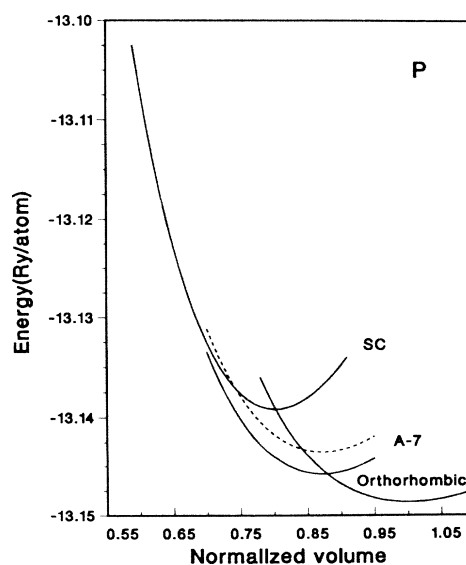


FIG. 4. Total crystal energy versus volume for the orthorhombic, *A*-7, and sc structures. Volumes are normalized by the calculated equilibrium volume for the orthorhombic structure. The dashed curve is the total energy of the *A*-7 phase shifted by 2.3 mRy per atom.

cubic (*A*-7) structures. Although black phosphorus and nitrogen³⁶ are formed in different structures than the other group-V elements at normal pressure, they behave like As, Sb, and Bi at high pressure. There is also structural similarity between the group-V elements and the group-(IV-VI) compounds which are stable in the NaCl (equivalent to the sc phase in the group-V) at zero temperature and the distorted NaCl (equivalent to the *A*-7 in the group-V) structures at room temperature.

Figure 4 shows the results for the total crystal energy calculations in black phosphorus as a function of volume for the orthorhombic, *A*-7, and sc phases. At zero pressure, the orthorhombic structure is found to be the most stable form and this is consistent with experiment. As pressure increases, the orthorhombic structure undergoes a phase transition into the *A*-7 phase. The calculated pressure for this transition is 30 kbar and this value is much smaller than the measured values which range from 40 to 80 kbar.¹⁻⁶ Since experimentally two phases of the orthorhombic and *A*-7 are mixed in this wide range of pressure, the transition pressure varies considerably even at room temperature.¹⁻⁶ The calculations show that the *A*-7 structure is stable in energy with respect to the sc phase up to a volume of $0.5V_0$ at zero temperature, where V_0 is the equilibrium volume. This fact is not consistent with experiment since the sc structure was found to be stable at room temperature and at pressures of about 110 kbar.^{1,3}

In Sec. VIA we have shown that the calculated ground-state properties for the three phases, orthorhombic, *A*-7, and sc, are in good agreement with the experiments. Therefore, the shapes of the total-energy curves in Fig. 4 are likely to be correct, and it is the cohesive energy differences between structures which differ from experiment. If the energies for the *A*-7 structure are increased by a constant for every volume, the *A*-7 to sc structural transition occurs in agreement with experiment. With a constant shift in the energy of 2.3 mRy per atom, the transition pressures and volumes are in excellent agreement with the experimental values³ obtained at room temperature (Table II). Hence, it may be reasonable to conclude that the agreement for both the orthorhombic to *A*-7 and *A*-7 to sc structural transitions suggests that the calculated crystal energies for the *A*-7 structure is slightly underestimated when compared to the room-temperature experimental data. The calculated 3.7% change of the volume at the *A*-7 to sc transition indicates that the transition is first order as found in experiment.³ In Sb, the same first-order transition was found with a 0.5% volume reduction.¹⁰

To confirm that the instability of the sc structure is a genuine result of our calculations, we tested other sets of k points for the sampling in the Brillouin zone and higher kinetic energy cutoff. We found the above results did not change. We also tested a different form of the exchange functional with the X_α ($\alpha=1$) approach.³⁷ In this case, the energy shift necessary to produce the correct transition pressure for *A*-7 to sc is about 3.3 mRy per atom, which is somewhat larger than our previous value.

It is interesting to compare the present results with other local-density-approximation calculations using

TABLE II. Comparison of the calculated transition pressures and volumes for the orthorhombic to *A*-7 and *A*-7 to sc phase transitions. Phases are distinguished by numbers 1 and 2. The total energy for the *A*-7 phase is shifted by 2.3 mRy per atom (see text). Volumes and pressures are in units of \AA^3 and kbar, respectively.

	V_1^1	V_2^1	$\Delta V/V_1^1$ (%)	P_t
Orthorhombic→ <i>A</i> -7				
Calc.	17.18	15.57	9.38	51.6
Expt. (Ref. 3)	16.82	15.10	10.2	55±5
<i>A</i> -7→sc				
Calc.	14.73	14.17	3.79	105
Expts.				
(Ref. 1)				111±9
(Ref. 3)	14.23	13.70	3.7	100±6

ab initio pseudopotentials. Calculations for group-(IV-VI) compounds have been successful in predicting the structural properties for the NaCl and distorted NaCl structures of SnTe (Ref. 25) and GeTe (Ref. 38). In both compounds, the rhombohedral NaCl structure was found to be stable at low temperature with respect to the NaCl phase and this agrees well with experiment. Although the above systems were not tested for structural stability under pressure, in the case of nitrogen³⁹ at high pressure, the *A*-7 structure is found to be stable with respect to the sc phase. Therefore, it appears that all the group-V elements are likely to form the *A*-7 structure relative to the sc structure.

The instability of the simple-cubic structure was recognized earlier by the elastic arguments based on the pairwise central forces⁴⁰ and by band-structure arguments related to the Jahn-Teller effect.¹² With increasing pressure, the previous pseudopotential calculation¹³ demonstrated that the lower electrostatic Madelung energy of the sc phase overshadows the decrease of the band-structure energy which favors the *A*-7 structure and thus the sc structure becomes stable at a more compressed volume. This agrees with our calculations since the structural differences between the *A*-7 and sc phases decrease with increasing pressure. However, this effect is found to be insufficient for stabilizing the sc structure. If the sc phase is stable as observed at room temperature, we suggest that additional mechanisms may be the larger zero-point energy correction to the *A*-7 structure, the large anharmonicity in the phonon couplings, or the strong electron-phonon interactions which favor high-temperature superconductivity^{6,7} for the sc structure.

Since the sc phase is not a dense-packing structure, closed-packed structures like body-centered cubic (bcc), face-centered cubic (fcc), and hexagonal-closed packed (hcp) are likely to be stable at higher pressure. The bcc structure was found at 280 kbar in Sb (Ref. 41) and 77 kbar in Bi (Ref. 42). In black phosphorus, however, we found no indication of such phase transitions into either bcc, fcc, or hcp. Our calculations showed that the total energy for the bcc structure is much higher than sc and the hcp structure is more stable than fcc. However, both the fcc and hcp structures have higher total energies than

bcc. Therefore, the sc structure is a very stable form in black phosphorus with respect to the closed-packed structures, bcc, fcc, and hcp, up to a pressure of 0.8 Mbar as observed in experiment.⁵

C. Valence charge distributions

Figure 5 shows the contour plots of the valence charge density for orthorhombic black phosphorus at zero pressure. As discussed in Secs. III and IV, the intralayer charge density has large peaked regions which represent the covalent bonds. These bonds are mainly composed of $3p$ orbitals since the $3s$ states are tightly bounded. In the region between layers, the bond charge density is much smaller than that associated with covalent bonds because of weak van der Waals interactions. The calculated charge densities are similar to those previously obtained using a pseudopotential approach.⁴³

The charge densities for the sc structure are drawn on the (100) and (110) planes in Fig. 6 at a pressure of 120 kbar which corresponds to an atomic volume of 14.0034 \AA^3 . Double humps appear between two adjacent atoms and the octahedral bonds are formed by three perpendicular p orbitals. When one of the interpenetrating lattices is displaced in the body diagonal direction by $\tau=0.236d$ corresponding to the minimum of the energy in Fig. 10, the structure loses its octahedral symmetry and three of the six first-neighbor distances become shorter by atomic displacement. Then, the charge density transfers into the

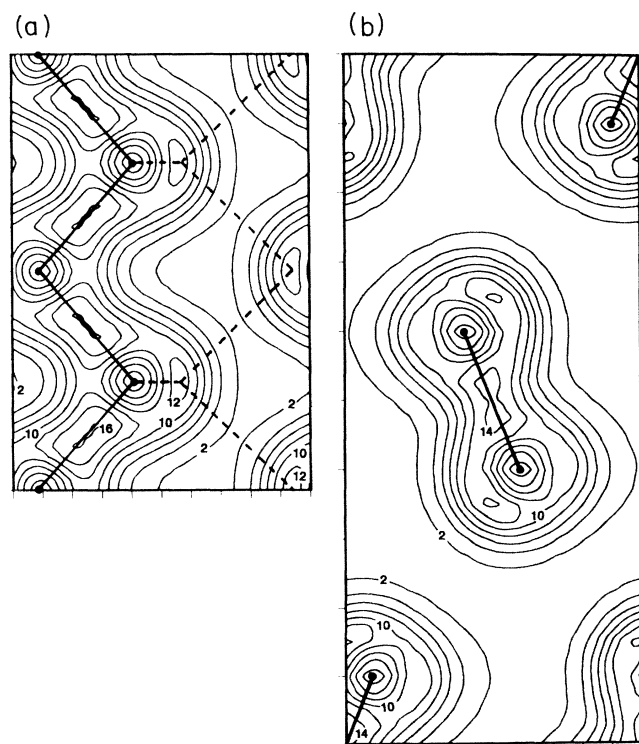


FIG. 5. Charge-density contour plots (a) in the (010) layer plane and (b) in the (100) plane showing the interlayer bonding in the orthorhombic structure at the calculated equilibrium volume. Steps are in units of two electrons per atomic volume.

compressed regions as shown in Fig. 6. The charge density averaged over the plane perpendicular to the $[111]$ direction (see Fig. 7) is commensurate with the longitudinal-acoustic (LA) wave at the zone corner $R(=\pi[1,1,1]/a)$ point in the Brillouin zone of the sc structure and resembles a one-dimensional Peierls distortion. These commensurate charge distributions split the energy degeneracies on the hexagonal faces of the fcc Brillouin zone. The energy separations near the Fermi level change a metallic state into a semimetallic state.

D. Band structures for the sc and displaced sc phases

In the group-(IV-VI) compounds,¹² the $A-7$ distortion of the rhombohedral shear and internal displacement changes the semimetallic structure into a semiconductor. Since sc black phosphorus is a metal at high pressure, the distortion induces the semimetallic transition. As shown in Fig. 8, degenerate energy levels of the sc structure are separated along the LW line in the hexagonal face of the fcc Brillouin zone. Along this axis, the charge decompositions show that the lowest two states are bonding and antibonding s states. The third and fourth bands are mainly p_z and p_y orbitals. Near the Fermi level, unsymmetric charge distributions in the octahedral bonds split the degenerate levels. We find that the fifth band has more p_x electrons resulting from the symmetry breaking than the sixth. Since the hexagonal face is perpendicular to the $[111]$ direction, the energy separations on this plane are very similar to those expected from a Peierls distortion. In the usual group-V elements As and Sb, the s -band width at the zone center is 5–10 eV and this band is well separated from the p -symmetry bands. We note that for phosphorous the band separation between s -bonding and s -antibonding states at the Γ point is 14.5 eV and the s -antibonding energy is very close to that of p bonding. The difference in the band structure of P is because the pressure is higher and thus the deep s orbitals are slightly delocalized.

The density of states for the sc phase is estimated to be 4.2 Ry/atom. The $A-7$ distortion makes a little dip in the density of states at the Fermi level and thus the band-structure energy is lowered. In the comparison between the total crystal energies for the sc and $A-7$ structures, the difference is found to be of the same order of magnitude as the band-structure energy difference.

E. Phonon frequencies along the $[111]$ axis

We have calculated the phonon frequency for the LA mode at the zone corner R point in the sc Brillouin zone. This phonon mode is particularly interesting since its atomic displacements correspond to the internal lattice movement from the sc to $A-7$ phases. In the sc structure, the atomic layers projected onto the (111) plane form hexagonal lattices as seen in Fig. 9. The phonon polarization for the LA mode at the zone corner corresponds to a Peierls-like distortion of the hexagonal planes in the $[111]$ direction. Figure 10 shows the change of the total energy as a function of displacement for this particular phonon mode. When atoms move in opposite directions with a displacement δd , the internal displacement of the lattice is

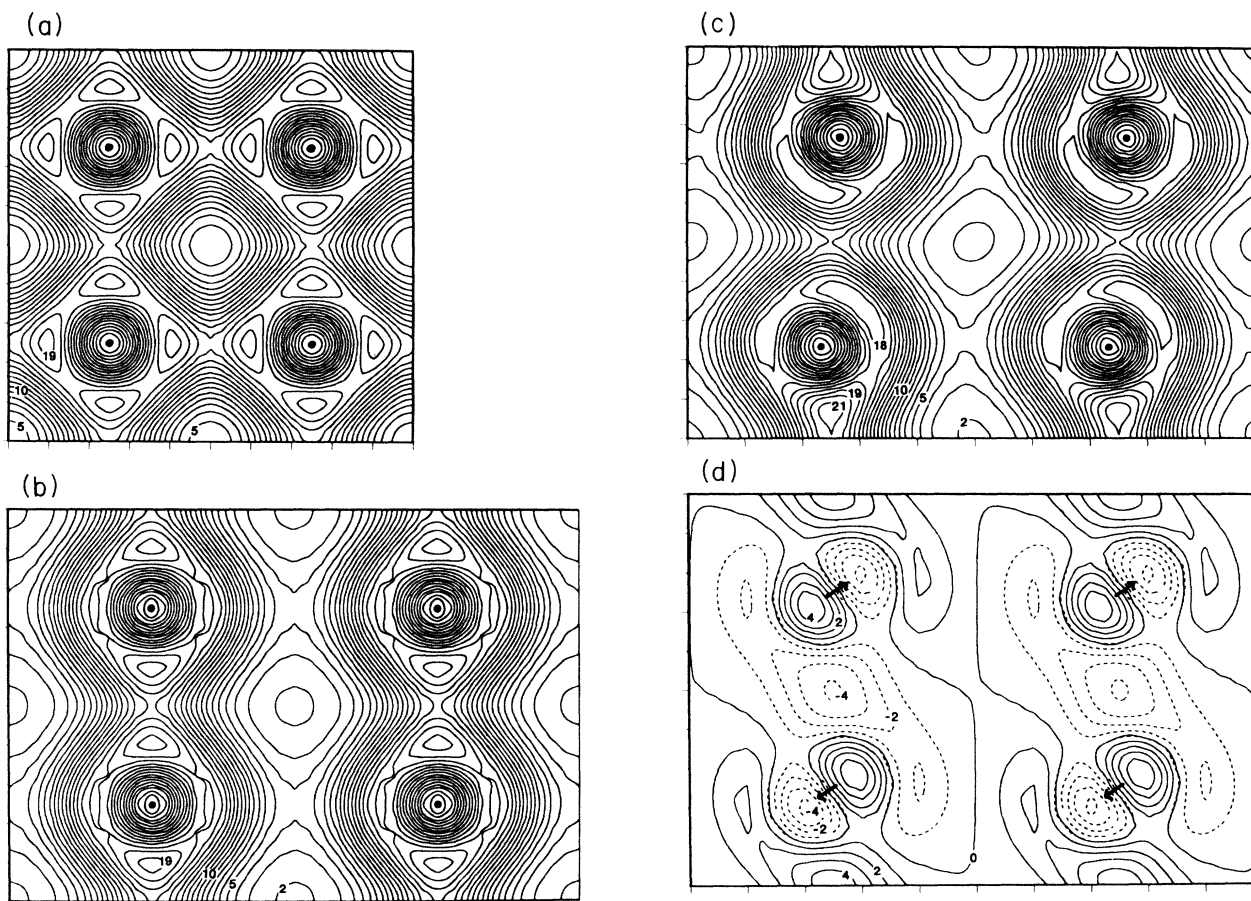


FIG. 6. Charge-density contour plots (a) in the (100) and (b) (110) planes for the sc phase. The contour plot of the displaced sc phase is in (c) and the difference between (b) and (c) is in (d). The primitive cell volume having two atoms is chosen to be 28.0068 \AA^3 and the internal displacement $u=0.236$. Dashed lines denote negative contours. Steps are in units of one electron per cell volume.

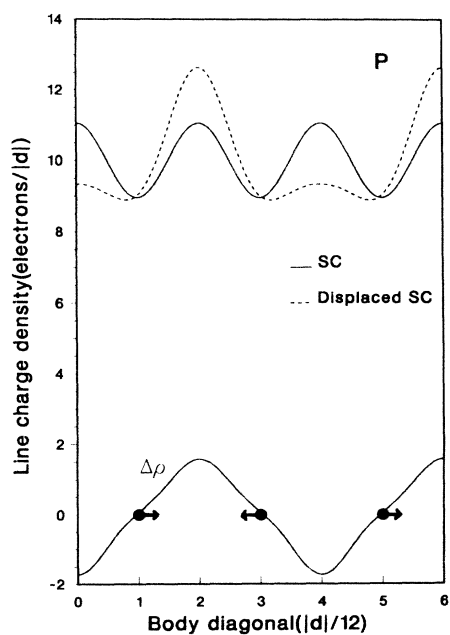


FIG. 7. Charge density averaged over the (111) plane for the sc and displaced sc phases. The difference is plotted at the bottom. Volume and displacement are the same as those used in Fig. 6. Arrows indicate the displacements of the hexagonal planes in Fig. 9.

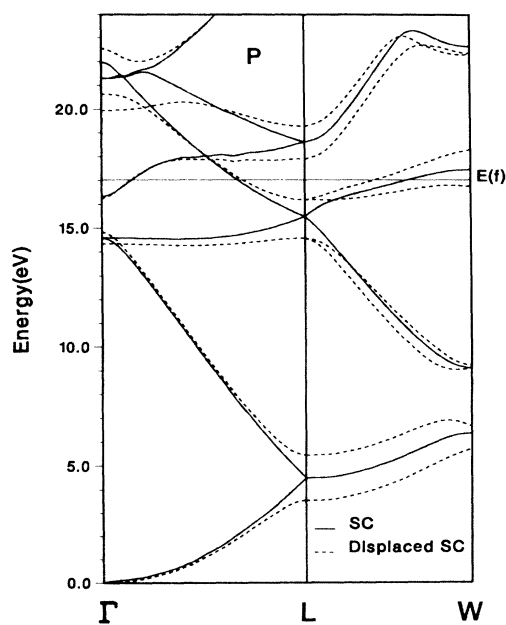


FIG. 8. Energy band structures for the sc and displaced sc phases. Volume and displacement are the same as those used in Fig. 6.

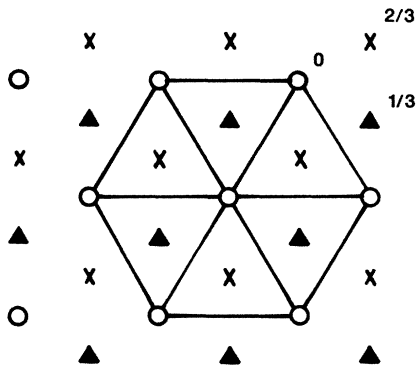


FIG. 9. Atomic lattices of the sc phase projected onto the (111) plane. Hexagonal planes are distinguished by different points. Numbers listed are the diagonal distances in units of $d/2$.

$u=0.25-\delta$. For smaller displacements, the energy decreases and thus the sc structure is destabilized. The curve has a minimum at a phonon displacement of $\delta_0=0.014$ and then $u=0.236$. If δ is less than δ_0 , the electronic part of the Hellmann-Feynman force with a positive value contributes more than the ionic part. Then, the force acting on an atom points to the phonon distortion and stabilizes the *A-7* structure against the displacement. Above δ_0 , the ionic force contributed by the Ewald energy is larger. When the rhombohedral angle α decreases from 60° , the minimum of the energy moves to a slightly higher value. Then, the structure gradually changes into the stable *A-7* structure.

Results are also shown (Fig. 10) for the transverse-acoustic mode. The calculated harmonic coefficients of the energy expansions for both the LA and TA modes are found to be $-0.23412 \text{ Ry}/(\text{a.u.})^2$. Thus, the phonon frequency is imaginary with a magnitude of 9.44 THz. Nitrogen in the sc structure is also found to have imaginary frequencies for the same phonon modes. This is equivalent to the unstable transverse-optic (TO) phonon frequency calculated at zero temperature at the zone center of SnTe and GeTe with the NaCl structure. With increasing pressure, the harmonic coefficient increases and is found to be zero at a volume of about $0.5V_0$. For this case, the distorted energy curve in Fig. 10 has no minimum. At the midpoint along the [111] direction, the LA phonon frequency is estimated to be 7.29 THz. Therefore, the phonon modes are very soft near the zone corner.

The fourth-order anharmonic coefficient represents the phonon-phonon interaction. Since atoms move according to the distortion of the LA mode, the fourth-order term of the expansion in Fig. 10 is the interaction Φ_{lll} between longitudinal-acoustic phonons. When the atomic polarizations are perpendicular to the [111] direction, we can calculate the interaction Φ_{llt} between longitudinal- and transverse-acoustic phonons. We find that a value of $\Phi_{lll}=56.5 \text{ Ry}/(\text{a.u.})^4$ and $\Phi_{llt}=\Phi_{lll}/3$. To compare the anharmonic terms of black phosphorus with those in sys-

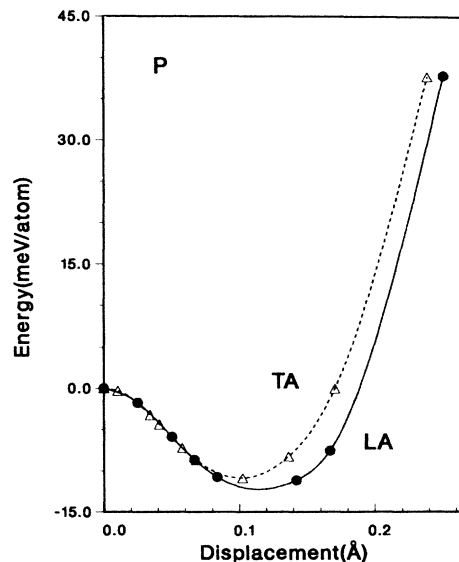


FIG. 10. Crystal energy change versus phonon displacement for the sc phase. The phonon modes chosen are the LA and TA modes at the zone corner *R* point of the sc Brillouin zone. The volume is the same as that used in Fig. 6.

tems of valence four, we tested the same phonon mode in simple-cubic Si. Because Si has sp^3 orbitals, the sc phase is stabilized against the displacement and the phonon frequency is real. The anharmonic coupling is negative and almost negligible. Therefore, the peculiar sc instabilities and unstable phonon modes at the zone corner in the group-V elements result from the octahedral bondings of $3p$ orbitals.

The phonon-phonon interactions between different k points are calculated by choosing atomic displacements as the combination of corresponding phonon polarizations.³¹ For simplicity, we choose the phonons at $\pi[1,1,1]/2a$ and $\pi[1,1,1]/a$. The calculated fourth-order term between longitudinal-acoustic phonons is $30 \text{ Ry}/(\text{a.u.})^4$; it has the same order of magnitude as Φ_{llt} at $\pi[1,1,1]/a$.

Anharmonic couplings play an important role at finite temperatures. The increase of the TO(Γ) phonon frequency with temperature stabilizes the NaCl structure of SnTe and GeTe. It was understood that the phase transition for these compounds results from strong electron-phonon interactions and anharmonic phonon-phonon interactions.^{44,45} Although all phonon-phonon interactions have not been calculated, the strong anharmonic couplings for particular modes indicate that temperature can be a possible origin of the sc phase stability at room temperature in highly condensed black phosphorus.

Because of a large electronic contribution to the force and soft phonon frequencies near the *R* point, the electron-phonon interactions are expected to be strong. In fact, the sc structure is found to be superconducting^{6,7} with a critical temperature from 6 to 10 K. Although the electron-phonon interactions influence the structural stability of the *A-7* and sc phases, quantitative comparison is beyond the scope of this paper.

V. CONCLUSION

We have shown that the pseudopotential-total-energy method can explain successfully the orthorhombic stability at normal pressure and the orthorhombic to *A-7* phase transition in black phosphorus. The *A-7* structure has been found to be very stable relative to the sc phase at zero temperature. The change of the sc energy band structure and the imaginary phonon frequency for the *A-7* lattice displacement confirm the stability for the *A-7* structure. Since the calculated equations of state are in good agreement with experiments for three different phases, orthorhombic, *A-7*, and sc, the only discrepancies from experiment are the relative cohesive energies when compared to room-temperature data. An *a priori* energy correction to the *A-7* crystal energy produces the transition pressures and volumes in excellent agreement with experiment. Moreover, the *A-7* stability relative to the sc structure is similar in the cases of black phosphorus and nitrogen at high pressure.

At this point, the physical origin of the energy correction for the *A-7* structure is not clear because of a lack of knowledge of the entire phonon spectrum and the specific heat at different pressure. However, qualitative explanations are possible based on the calculated soft phonon modes and strong phonon-phonon interactions for particular phonon modes considered here. The zero-point energy, temperature change of the free energy, and electron-

phonon interaction can be corrections to the underestimation of the energy of the *A-7* structure. The thermal expansion due to an increase of temperature should be small because its effect increases the discrepancy from the sc phase. On the other hand, detailed x-ray experiments for the superconducting phases⁴⁶ are necessary to determine whether it is a pure sc or a mixture of phases of unknown structure at very low temperature. Recent experiments⁶ performed at low temperatures have indicated a possible mixture of several phases. Finally, we suggest that a determination of the phase boundary^{3,47} between pressure and temperature down to liquid-helium temperature is valuable to see the change of the transition pressure.

ACKNOWLEDGMENTS

We would like to thank Dr. J. Wittig for discussions and data. We would also like to thank Professor L. M. Falicov and Professor S. G. Louie for helpful comments and discussions, and Dr. S. Froyen for his help with the force program. This work was supported by U.S. National Science Foundation Grant No. DMR8319024 and by the Director, Office of Energy Research, Office of Basic Energy Sciences, Materials Science Division of the U.S. Department of Energy under Contract No. DE-AC03-76SF00098. CRAY computer time was provided by the Office of Energy Research of the Department of Energy.

¹J. C. Jamieson, *Science* **139**, 1291 (1963).

²A. Brown and S. Rundquist, *Acta. Crystallogr.* **19**, 684 (1965).

³T. Kikegawa and H. Iwasaki, *Acta. Crystallogr. Sect. B* **39**, 158 (1983).

⁴L. Cartz, S. R. Srinivasa, R. J. Riedner, J. D. Jorgensen, and T. G. Worton, *J. Chem. Phys.* **71**, 1718 (1979).

⁵M. Okajima, S. Endo, Y. Akahama, and S. Narita, *Jpn. J. Appl. Phys.* **23**, 15 (1984).

⁶H. Kawamura, I. Shirovani, and K. Tachikawa, *Solid State Commun.* **49**, 879 (1981); **54**, 775 (1985).

⁷J. Wittig, B. Bireckoven, and T. Weidlich, *Solid State Physics Under Pressure: Recent Advance with Anvil Devices*, edited by S. Minomura (Reidel Dordrecht, 1985), p. 217.

⁸L. M. Falicov and S. Golin, *Phys. Rev.* **137**, A871 (1965).

⁹W. B. Pearson, *A Handbook of Lattice Spacings and Structures of Metals and Alloys*, (Pergamon, New York, 1958), Vol. 2, p. 816; W. H. Beamer and C. R. Maxwell, *J. Chem. Phys.* **17**, 1293 (1949).

¹⁰T. N. Kolobyanina, S. S. Kabalkina, L. F. Vereshchagin, and L. V. Fedina, *Zh. Eksp. Teor. Fiz.* **55**, 164 (1968) [*Sov. Phys.—JETP* **28**, 88 (1969)].

¹¹R. M. Brugger, R. B. Bennion, and T. G. Worlton, *Phys. Lett.* **24A**, 714 (1967).

¹²M. H. Cohen, L. M. Falicov, and S. Golin, *IBM. J. Res. Dev.* **8**, 215 (1964).

¹³D. Schiferl, *Phys. Rev. B* **19**, 806 (1979).

¹⁴M. L. Cohen, *Phys. Scr.* **T1**, 5 (1982).

¹⁵P. Hohenberg and W. Kohn, *Phys. Rev.* **136**, B864 (1964); W. Kohn and L. J. Sham, *ibid.* **140**, A1133 (1965).

¹⁶E. Wigner, *Trans. Faraday Soc.* **34**, 678 (1938).

¹⁷M. T. Yin and M. L. Cohen, *Phys. Rev. B* **24**, 6121 (1981).

¹⁸M. T. Yin and M. L. Cohen, *Phys. Rev. B* **26**, 5668 (1982).

¹⁹S. Froyen and M. L. Cohen, *Phys. Rev. B* **28**, 3258 (1983).

²⁰J. Ihm and J. D. Joannopoulos, *Phys. Rev. B* **24**, 4191 (1981).

²¹K. J. Chang and M. L. Cohen, *Solid State Commun.* **50**, 487 (1984).

²²K. J. Chang and M. L. Cohen, *Phys. Rev. B* **30**, 4774 (1984).

²³S. Froyen and M. L. Cohen, *Phys. Rev. B* **29**, 3770 (1984); unpublished.

²⁴D. R. Hamann, M. Schlüter, and C. Chiang, *Phys. Rev. Lett.* **43**, 1494 (1979).

²⁵K. M. Rabe and J. D. Joannopoulos, *Phys. Rev. B* **32**, 2302 (1985).

²⁶J. Ihm, A. Zunger, and M. L. Cohen, *J. Phys. C* **12**, 4401 (1979).

²⁷K. J. Chang and M. L. Cohen, *Phys. Rev. B* **31**, 7819 (1985).

²⁸P. K. Lam and M. L. Cohen, *Phys. Rev. B* **25**, 6139 (1982).

²⁹H. Hellmann, *Einführung in dir Quanten Theorie* (Deuticke, Leipzig, 1937), p. 285; R. P. Feynman, *Phys. Rev.* **56**, 340 (1939).

³⁰F. D. Murnaghan, *Proc. Nat. Acad. Sci. U.S.A.* **30**, 244 (1944).

³¹M. T. Yin and M. L. Cohen, *Phys. Rev. B* **26**, 3259 (1982).

³²D. Vanderbilt, S. G. Louie, and M. L. Cohen, *Phys. Rev. Lett.* **53**, 1477 (1984).

³³M. T. Yin and M. L. Cohen, *Phys. Rev. B* **29**, 6996 (1984).

³⁴See references in P. B. Littlewood, *J. Phys. C* **13**, 4875 (1980).

³⁵J. C. Phillips, *Bonds and Bands in Semiconductors* (Academic, New York, 1973).

³⁶D. Schiferl, S. Buchsbaum, and R. L. Mills, *J. Phys. Chem.* **89**, 2324 (1985).

³⁷J. C. Slater, *Phys. Rev.* **81**, 385 (1951).

- ³⁸We have calculated the structural properties for GeTe. The lattice constant and bulk modulus are in good agreement with experiment. The NaCl structure is found to be unstable with respect to the rhombohedral NaCl structure at zero temperature.
- ³⁹See references in R. Reichlin, D. Schiferl, S. Martin, C. Vanderborgh, and R. Mills, *Phys. Rev. Lett.* **55**, 1464 (1985); we also calculated the total energies for the *A*-7 and sc nitrogen and found that the *A*-7 crystal energy is lower than sc as seen in black phosphorus considered here.
- ⁴⁰M. Born and K. Huang, *Dynamical Theory of Crystal Lattices* (Oxford University Press, London, 1954).
- ⁴¹K. Aoki, S. Fujiwara, and M. Kusakabe, *Solid State Commun.* **45**, 161 (1983).
- ⁴²K. Aoki, S. Fujiwara, and M. Kusakabe, *J. Phys. Soc. Jpn.* **51**, 3826 (1982).
- ⁴³H. Asahina, K. Shindo, and A. Morita, *J. Phys. Soc. Jpn.* **51**, 1193 (1982).
- ⁴⁴H. Kawamura, *Narrow Gap Semiconductors: Physics and Applications*, Vol. 133 of *Lecture Notes in Physics*, edited by W. Zawadski (Springer, Berlin, 1980), p. 470.
- ⁴⁵A. Natori, *J. Phys. Soc. Jpn.* **41**, 782 (1976).
- ⁴⁶J. Wittig and B. T. Matthias, *Science* **160**, 994 (1968).
- ⁴⁷C. W. F. T. Pistorius, *Prog. Solid State Chem.* **11**, 1 (1976); C. G. Homan, *J. Phys. Chem. Solids* **36**, 1249 (1975).